Supplementary Information

Identification of novel LRRK2 inhibitors by structure-based virtual screening and alchemical free energy calculation

Shuoyan Tan[a], Xiaoqing Gong[b], Huanxiang Liu[b*], Xiaojun Yao[b*]

[a] College of Chemistry and Chemical Engineering, Lanzhou University, Lanzhou 730000, China

[b] Faculty of Applied Sciences, Macao Polytechnic University, 999078, Macao SAR, China

Corresponding authors

Huanxiang Liu Tel: +853-8599-6874; Email: hxliu@mpu.edu.mo

Xiaojun Yao Tel: + 853-8599-6487; Email: xjyao@mpu.edu.mo

Data Availability Statement

The data for this article, including the detailed results of each AFE simulation analyzed by the pymbar program (Fig. 5 and Figs S4, S5, S6 and S7) are available at GitHub at https://github.com/tanshy17/Identification-of-novel-LRRK2-inhibitors-by-SBVS-and-AFE-calculation.

Supplementary Tables

Table S1. The inhibitor's index and experimental activity in test dataset

Target	series	Compound ID[a]	G2019S IC_{50}/K_i [b]	ΔG_{exp} [c]
LRRK2	PF	9	28.00	−10.36
		10	64.00	−9.87
		11	325.00	−8.90
		12	15.00	−10.73
		13	151.00	−9.36
		14	11.00	−10.92
		15	5223.00	−7.25
	MLI2	1	0.76	−12.51
		4	904.00	−8.29
		7	98.00	−9.62
		8	12.00	−10.87
		10	134.00	−9.43
		17	0.70	−12.56
		20	2.70	−11.76
		21	2.60	−11.78
		24	7.20	−11.17
		25	1.90	−11.97
	4YZN	2	6.00	−11.28
		9	11.00	−10.92
		10	20.00	−10.56
		11	6.00	−11.28
		12	33.00	−10.26
		14	7.00	−11.19
		15	3.00	−11.69
		16	13.00	−10.82
		17	1.00	−12.35
		18	71.00	−9.81
		19	1.00	−12.35
		20	13.00	−10.82
CHK1	CHK	17	72.00	−9.80
		19	520.00	−8.62
		20	170.00	−9.29
		21	190.00	−9.22
		22	5.00	−11.39
		33	1500.00	−7.99

a Compound ID corresponds to the molecular number in the original reference.

b IC_{50} and K_i values at the protein level are derived from the references. Unit: nM.

c ΔGexp is calculated from the experimental IC_{50} and Ki values using the equation: $\Delta G_{bind} = RT \cdot \ln K_i \approx RT \cdot \ln IC_{50}$, where T = 300.0 K. Unit: kcal/mol.

Table S2. Inhibition of compound LY2019-001 towards G2019S LRRK2 at various concentrations by Caliper MSA methods in previous SBVS work.

Compound conc. (nM)	Log con.	%inhibition1	%inhibition2	Average %inhibition
100000.00	5.00	60.29	55.78	58.04
50000.00	4.70	58.29	60.29	59.29
25000.00	4.40	52.28	54.28	53.28
12500.00	4.10	51.78	52.28	52.03
6250.00	3.80	51.28	55.78	53.53
3125.00	3.49	52.28	55.78	54.03
1562.50	3.19	51.28	50.78	51.03
781.25	2.89	53.78	55.78	54.78
390.63	2.59	52.28	61.29	56.79
195.31	2.29	59.79	58.29	59.04

The curve fitting is shown in Figure S9

The square filled with grey indicates that the concentration of the compound in intermediate dilution is poorly soluble.

Table S3. Inhibition of compound LY2019-001 towards WT LRRK2 at various concentrations by Caliper MSA methods in previous SBVS work

Compound conc. (nM)	Log con.	%inhibition1	%inhibition2	Average %inhibition
100000.00	5.00	64.74	43.68	54.21
50000.00	4.70	56.32	62.63	59.47
25000.00	4.40	40.53	52.11	46.32
12500.00	4.10	48.95	38.42	43.68
6250.00	3.80	51.05	56.32	53.68
3125.00	3.49	44.74	53.16	48.95
1562.50	3.19	46.84	40.53	43.68
781.25	2.89	61.58	53.16	57.37
390.63	2.59	46.84	58.42	52.63
195.31	2.29	60.53	40.53	50.53

The curve fitting is shown in Figure S9

The square filled with grey indicates that the concentration of the compound in intermediate dilution is poorly soluble.

Table S4. Inhibition of compound LY2023-001 towards G2019S LRRK2 at various concentrations by Caliper MSA methods in this work.

Compound conc. (nM)	Log con.	%inhibition1	%inhibition2	Average %inhibition
1000.00	3.00	77.85	77.76	77.81
500.00	2.70	89.30	83.70	86.50
250.00	2.40	87.57	79.66	83.61
125.00	2.10	84.94	85.90	85.42
62.50	1.80	78.98	83.46	81.22
31.25	1.49	66.99	68.33	67.66
15.63	1.19	44.25	49.02	46.64
7.81	0.89	28.66	32.86	30.76
3.91	0.59	12.19	9.03	10.61

Table S5. Predicted RBFEs of our designed compounds (LY2023-001 to LY2023-005) calculated by six estimators

	TI		TI-CUBIC		DEXP		IEXP		BAR		MBAR	
	avg	SD	avg	SD	avg	SD	avg	SD	avg	SD	avg	SD
ΔΔG LY2023-001	−1.91	0.10	−1.91	0.10	−2.21	0.10	−1.61	0.09	−1.81	0.06	−1.65	0.10
ΔΔG LY2023-002	−1.67	0.08	−1.67	0.08	−1.84	0.09	−1.51	0.08	−1.53	0.04	−0.94	0.06
ΔΔG LY2023-003	−1.28	0.10	−1.27	0.10	−1.47	0.10	−1.10	0.09	−1.20	0.05	−0.97	0.09
ΔΔG LY2023-004	0.19	0.13	0.20	0.13	0.53	0.13	−0.14	0.12	0.12	0.07	0.62	0.09
ΔΔG LY2023-005	4.06	0.19	4.06	0.19	5.38	0.18	2.54	0.20	4.80	0.08	3.52	0.13

pymbar program (https://github.com/MobleyLab/alchemical-analysis) was used to calculated the RBFE.

Table S6. Calculated relative binding free energies and the detailed contribution of different energy terms by the MM-GBSA method and AFE methods.

Methods		G2019S LY2023-001	G2019S LY2023-005
MMGBSA	ΔE_{ele}	−38.27	−11.33
	ΔE_{vdw}	−54.82	−26.77
	ΔE_{MM}[a]	−93.09	−38.09
	ΔG_{SA}	−6.69	−3.30
	ΔG_{GB}	49.80	23.26
	ΔG_{sol}[b]	43.11	19.95
	ΔG_{polar}[c]	11.53	11.93
	$\Delta G_{nonpolar}$[d]	−61.51	−30.07
	$\Delta H_{(GB)}$	−49.98	−18.14
	-TΔS	−22.32	−18.11
	ΔG_{bind}	−27.65	−0.03
experiment	IC_{50}(nM)[e]	12.90	11800.00
	ΔG_{exp}[f]	−10.75(0)	−6.72(4.03)
AFE[g] (kcal/mol)	TI	0	5.14
	TI-CUBIC	0	5.07
	DEXP	0	5.99
	IEXP	0	4.14
	BAR	0	4.96
	MBAR	0	3.77

a $\Delta E_{MM} = \Delta Eele + \Delta Evdw$.

b $\Delta Gsol = \Delta G_{GB} + \Delta G_{SA}$.

c $\Delta Gpolar = \Delta Eele + \Delta G_{GB}$.

d $\Delta Gnonpolar = \Delta Evdw + \Delta G_{SA}$.

e Caliper MSA In vitro activity of inhibitor in wild-type and G2019Smutation.

f Calculated by the experimental IC_{50} according to the equation ΔGbind = RT ln Kd ≈ RT ln IC_{50}, where T=300.0 K. units: kcal/mol.

g The relative binding free energies (RBFE) calculated by the Alchemical Free Energy (AFE) method, with molecule LY2023-001 serving as the reference compound and its binding free energy set to zero.

Table S7. Occupancy rates of hydrogen bonds between LRRK2 and two inhibitors (LY2023-005 and LY2023-001).

System	Acceptor	DonorH	Donor	Occupancy Rate
LY2023-001	MOL@N1	ALA_1950@H	ALA_1950@N	99.57%
	GLU_1948@O	MOL@H3	MOL@N6	89.78%
	ALA_1950@O	MOL@H1	MOL@N2	83.15%
	MOL@O1	ASP_2017@H	ASP_2017@N	59.29%
	MOL@O1	LYS_1906@HZ3	LYS_1906@NZ	31.30%
LY2023-005	MOL@N1	ALA_1950@H	ALA_1950@N	97.12%
	ALA_1950@O	MOL@H2	MOL@N2	71.46%

GLU_1948@O	MOL@H1	MOL@N5	64.92%

The table lists hydrogen bonds with occupancies greater than 30 %.

Supplementary Figures

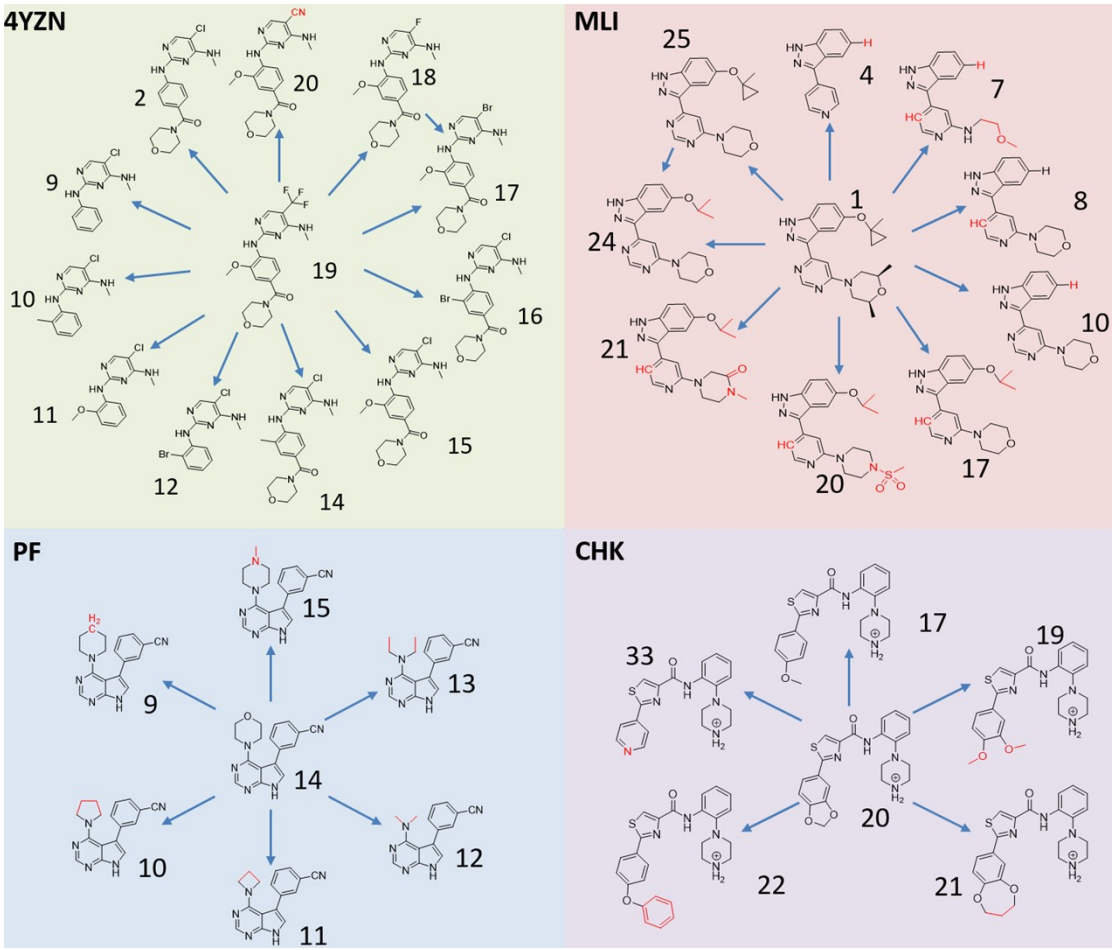

Figure S1. The transition maps for the 35 ligands in the test dataset. Atoms requiring transformation are highlighted in red. The numbers are the compound ID in Table S1.

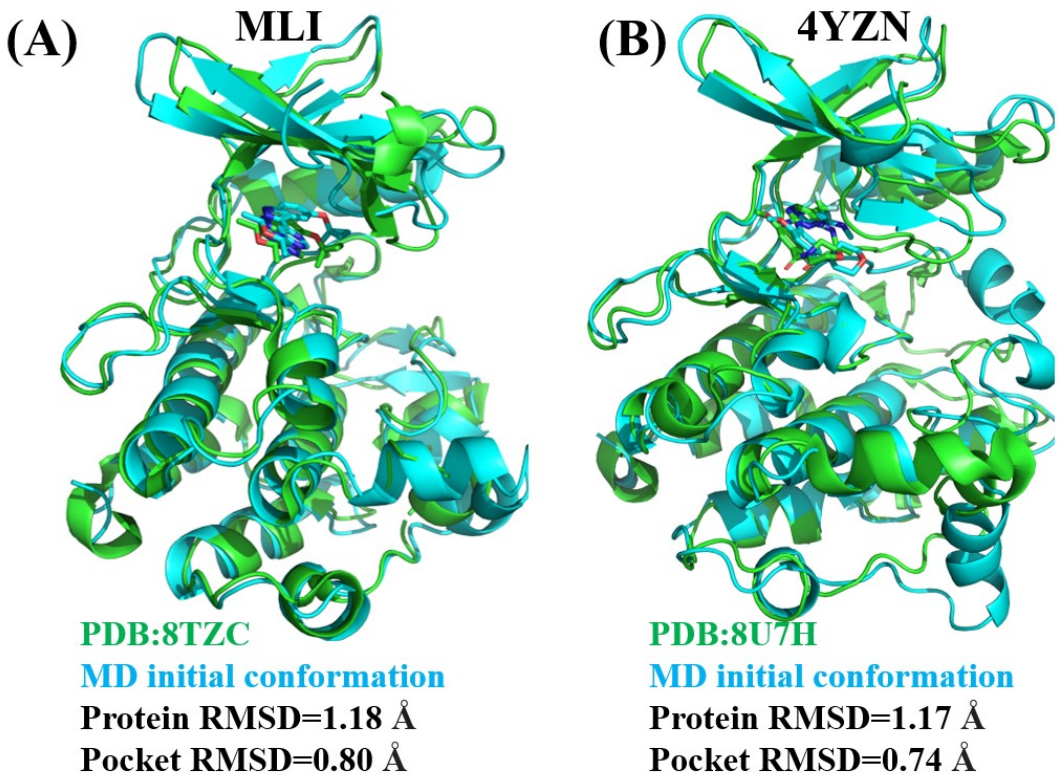

Figure S2. Comparison of experimental complex structures with the initial conformations used in alchemical simulations. (A) Alignment of the electron microscopy structure of G2019S LRRK2 in complex with type I inhibitor MLI-2 (PDB: 8TZC, in green) and the initial conformation of the MLI series utilized in alchemical simulations (in blue). (B) Alignment of the electron microscopy structure of G2019S LRRK2 bound to type I inhibitor GNE-7915 (PDB: 8U7H, in green) and the initial conformation of the 4YZN series employed in alchemical simulations (in blue). Protein RMSD calculations are performed using residues within the sequence range of 1879-2138. Pocket RMSD calculations are conducted based on residues located within 5 Å of the small molecule.

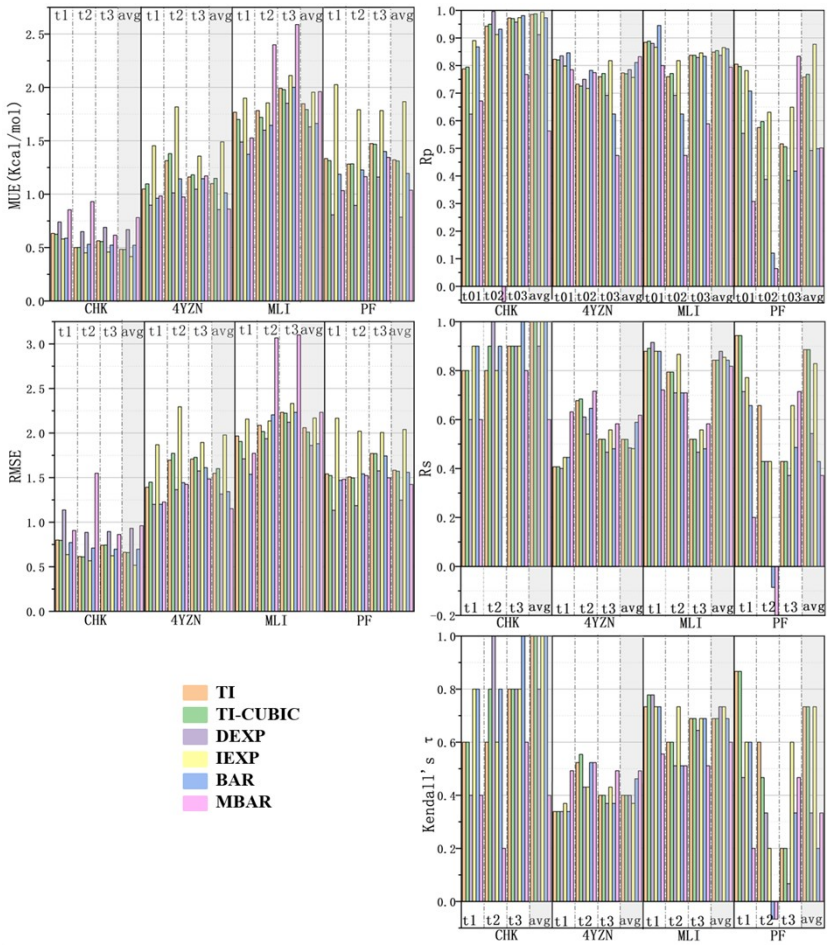

Figure S3. Accuracy (MUE, RMSE) and correlation (Rp, Rs, τ) for individual simulations (t1, t2, and t3) and the average of three simulations (avg).

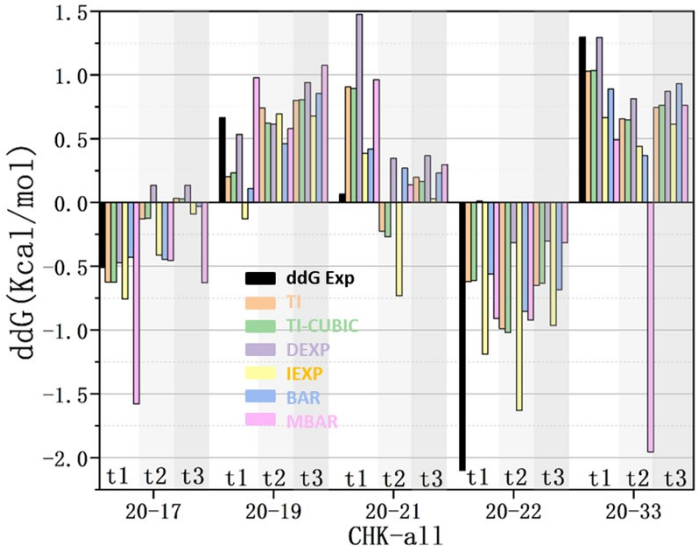

Figure S4. Predictive results for CHK1 kinase inhibitors with an arylamide scaffold (CHK series) in each simulation (t1, t2, t3). Black bars denote the experimental relative binding free energies, and colored bars show the relative binding free energies as calculated by different alchemical

estimators.

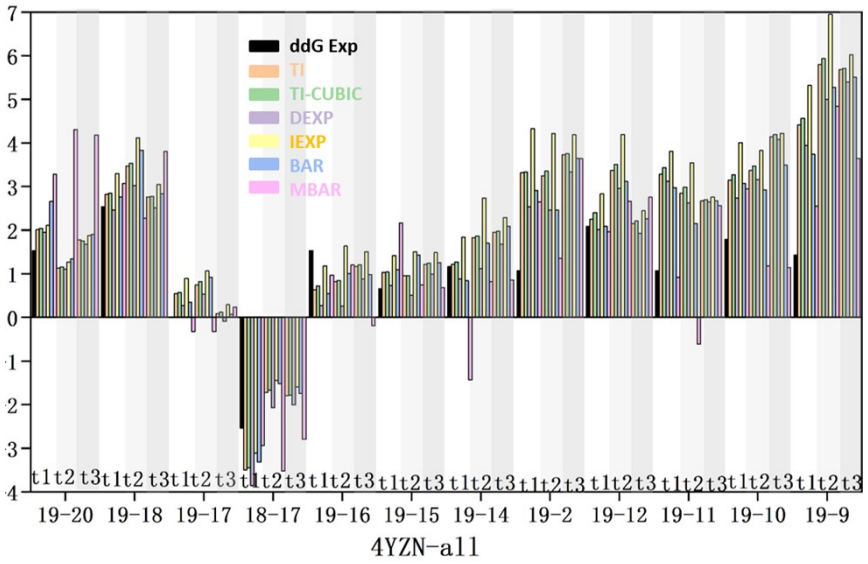

Figure S5. Predictive results for LRRK2 kinase inhibitors with an aminopyrimidine scaffold (4YZN series) in each simulation (t1, t2, t3).

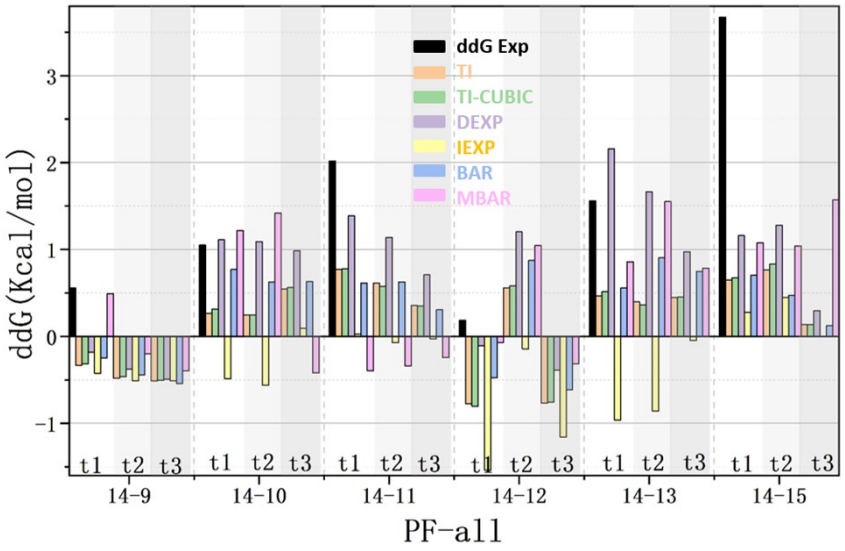

Figure S6. Predictive results LRRK2 kinase inhibitors with a pyrrolopyrimidine scaffold (PF series) in each simulation (t1, t2, t3).

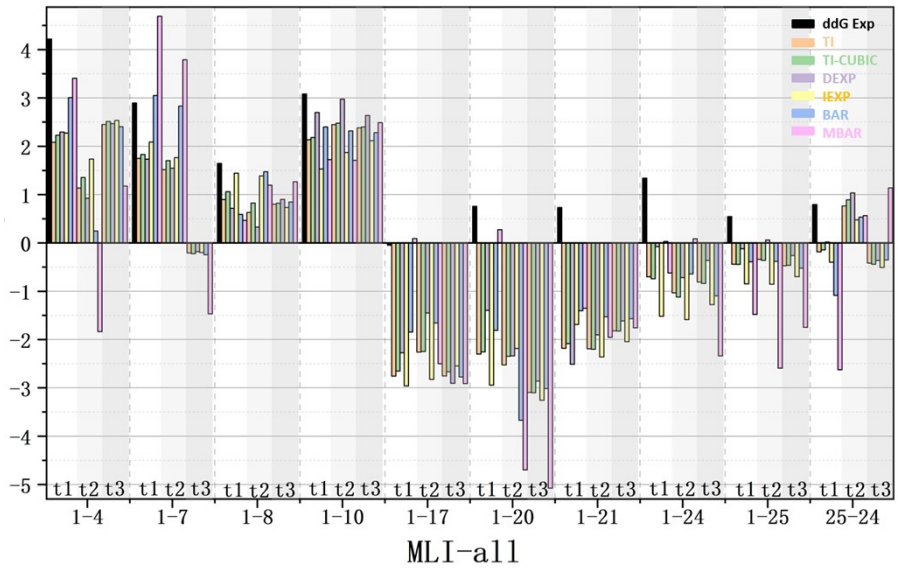

Figure S7. Predictive results for LRRK2 kinase inhibitors with an indazole MLI scaffold (MLI series) in each simulation (t1, t2, t3).

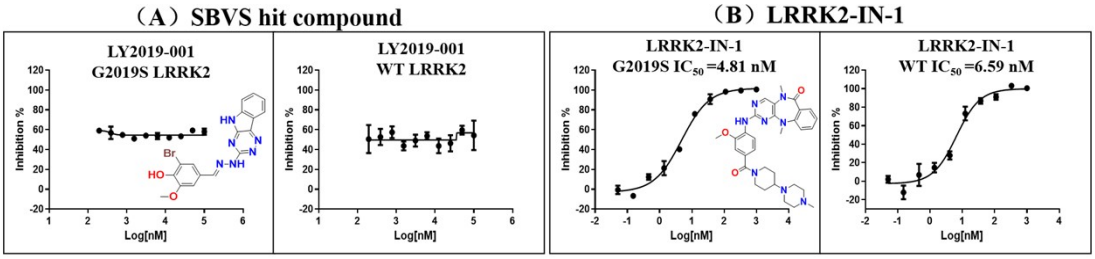

Figure S8. Kinase inhibition assays using the Caliper MSA method. (A) IC_{50} of compound LY2019-001 toward the G2019S mutant and WT LRRK2, determined in pervious SBVS work. (B) IC_{50} values of Positive control LRRK2-IN-1 against WT and G2019S mutant LRRK2, determined in pervious SBVS work.

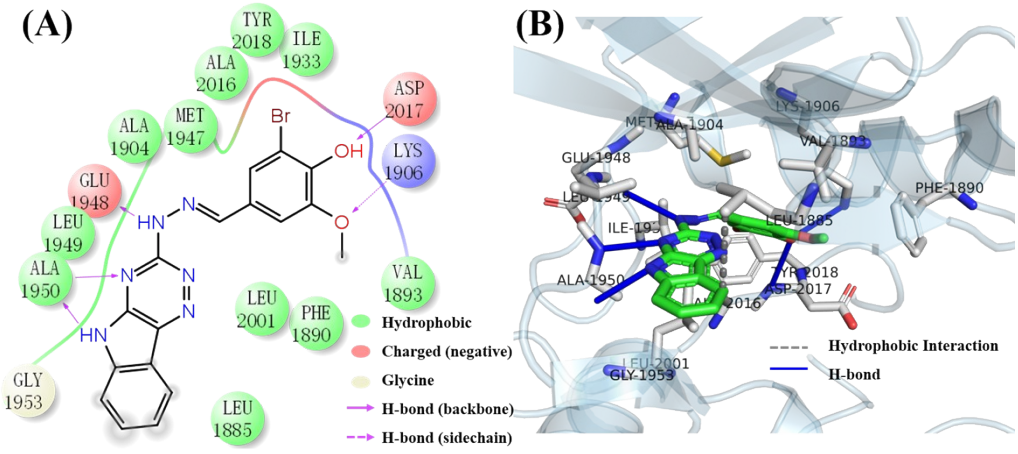

Figure S9. Binding mode between LY2019-001 and G2019S LRRK2. Molecular docking suggests two potential binding modes for compound LY2019-001 with its target. The most probable binding mode was determined through MD simulations and MM-GBSA free energy calculations, as illustrated in this figure.